ESTIMATING ENHANCED FUJITA SCALE LEVELS BASED ON FOREST DAMAGE SEVERITY

Christopher M. Godfrey*
University of North Carolina at Asheville, Asheville, North Carolina

Chris J. Peterson
University of Georgia, Athens, Georgia

1. INTRODUCTION

Enhanced Fujita (EF) scale estimates following tornadoes remain challenging in rural areas with few traditional damage indicators. In some cases, traditional ground-based tornado damage surveys prove nearly impossible, such as in several 27 April 2011 long-track tornadoes that passed through heavily forested and often inaccessible terrain across the southern Appalachian Mountains. One tornado, rated EF4, traveled 18 miles over the western portion of the Great Smoky Mountains National Park (GSMNP) in eastern Tennessee. This tornado received its rating based on a single damage indicator—the tornado collapsed a metal truss tower along an electrical transmission line (NWS Morristown 2011, personal communication). Although the upper bound for this particular damage indicator is near the peak of the range of wind speeds corresponding with an EF3 rating, the surveyor noted the incredible damage to the trees in the area and decided to augment the rating to an EF4. A second tornado, rated EF3, traveled 38 miles across the mountains of northern Georgia in the Chattahoochee National Forest (CNF). This tornado received its rating based on damage to numerous structures near the very end of its long path. In both cases, the vast majority of the tornado track remained inaccessible to surveyors. These rare and notable events provide a unique and valuable opportunity to assess tornadic winds in heavily forested and mountainous areas through analyses of forest damage.

Research on observed tornado behavior in rough terrain remains limited in the peer-reviewed literature. Fujita (1989) analyzes damage from a violent tornado in the forested mountainous terrain of northwest Wyoming. Dunn and Vasiloff (2001) examine the Doppler radar presentation of a tornado in Salt Lake City. Bluestein (2000) analyzes a tornado in the high terrain of Colorado and addresses the need for future research that studies the role of orography and elevation in modifying the behavior of supercells over mountainous terrain. LaPenta et al. (2005) and Bosart et al. (2006) review case studies of tornadoes in complex terrain in eastern New York and western Massachusetts, respectively, and pose the question of how terrain-channeled low-level flow influences the mesoscale environment and tornadogenesis. Both Bluestein (2000) and Bosart et al. (2006) suggest that further numerical simulations of the supercellular and low-level environment are warranted. Indeed, numerous authors use numerical simulations to study near-surface tornado dynamics (e.g., Dessens 1972; Fiedler 1994; Fiedler and Rotunno 1986; Lewellen and Lewellen 2007; Lewellen et al. 1997, 2000, 2008), but only recently has anyone attempted to incorporate very simple terrain variations into such models (e.g., D. Lewellen 2012, personal communication). Thus, observational studies that characterize the near-surface tornadic wind field in complex topography remain vitally important.

Previous studies of tornado tracks through forests (e.g., Bech et al. 2009; Beck and Dotzek 2010; Blanchard 2013) suggest that the orientation and degree of damage of fallen trees will allow a reconstruction of the near-surface wind field. Letzmann (1925) presents the original foundation for this type of analysis and derives predictions of surface-level wind fields based on analytical solutions to simple Rankine vortex events. By assuming that trees fall in the direction of the wind at the moment the force exceeds their rooting or trunk strength, Letzmann (1925) notes that the spatial pattern of fallen trees, and their orientations, preserves a signature of the surface-level winds as a tornado moves over a forested landscape. More recently, Holland et al. (2006) combine Letzmann's (1925) wind field model with forestry mod-

FIG. 1. A sample of an aerial photograph showing individual tree trunks, crowns, and root balls. Similar imagery covers the entire 56-mile length of both tornado tracks.

*Corresponding author address: Christopher M. Godfrey, University of North Carolina at Asheville, Department of Atmospheric Sciences, 1 University Heights, Asheville, North Carolina 28804-8511; e-mail: cgodfrey@unca.edu.

els of tree stability developed by Peltola and Kellomaki (1993) for European trees (i.e., Norway spruce). Holland et al. (2006) modify the tree stability model with parameters for loblolly pine in the southeastern United States and produce hypothetical forest damage patterns from a simulated tornado, though the authors did not have the opportunity to compare the predicted damage patterns with empirical observations. Bech et al. (2009) examine actual tree damage patterns and compare them to classes of Letzmann's (1925) predictions, but do not include a tree stability component, thereby implicitly assuming a homogeneous stand of trees. Beck and Dotzek (2010) more fully develop this approach by examining actual tree damage patterns after two European tornadoes, using simulated vortices and the Peltola and Kellomaki (1993) tree stability model. Using this approach, the authors infer wind field parameters for the two tornadoes, demonstrating, for example, the temporal evolution of intensity along the tornado track. Karstens et al. (2013) used the Beck and Dotzek (2010) approach to produce similar estimates of tornado intensity based on analyses of treefall patterns in two tornadoes, but used the thresholds for damage in the EF scale to create a distribution of critical wind speeds necessary to blow down trees. Godfrey and Peterson (2012) also attempted to use the Beck and Dotzek (2010) approach, combined with a tree stability model (Peltola and Kellomaki 1993), to characterize the near-surface wind field through rugged terrain for the same two subject tornadoes under scrutiny in this study. While this method shows great promise in relatively flat areas, unpublished research efforts by the present authors indicate that the approach will not work in regions with complex topography.

The present work therefore describes a novel method to infer EF-scale levels from forest damage using the degree of tree damage and a coupled wind and tree resistance model. This new approach remains independent of the source of the wind. Its wind speed estimates therefore apply to any type of wind damage.

2. DATA

2.1 *Aerial imagery*

Sixty-four days after the tornado outbreak, a chartered flight captured aerial photographs along the entire length of both tornado tracks. The plane made two passes along each track, giving a total composite image width of about 1500 m (5000 feet) with a nominal pixel resolution of eight inches. These high-resolution, georeferenced images show individual tree trunks, crowns, and root balls (Fig. 1). Each of the 130,000 downed trees shown in the imagery received a label marking its geographic coordinates and fall direction. Nearby standing trees also received tags showing their geographic coordinates. Together, over 448,000 fallen and standing trees received labels.

2.2 *Ground Surveys*

Ground surveys provide valuable information that is unobtainable from the air. The authors recorded details on each tree within 400 m^2 plots in each tornado track, including the tree species, diameter at breast height (DBH), fall direction, snap heights, whether or not the tree remains alive, and the damage type. Damage types include "branches broken," "crown broken," "snapped," "bent," "leaning," "uprooted," and "intact." Through 2012, the surveys collected information on 1551 individual trees in 69 plots in the CNF tornado track and 503 individual trees in 22 plots in the GSMNP track. Tree heights for a small selection of trees in the CNF tornado track were measured in a variety of ways, depending on tree size and position. One method utilizes a telescoping fiberglass pole that can measure the height of relatively short trees. Another option involves a simple tape measure to determine the height of uprooted trees on the ground. For trees that have snapped, the total height is the sum of the height of the stump and the length of the remaining nearby trunk and crown. Other options include an optical rangefinder and simple geometry. The following analysis assumes that the samples obtained in the ground surveys represent the species composition and size distribution of the trees in each respective forest.

3. METHODOLOGY

For each tornado track, a statistical resampling procedure begins by randomly drawing, with replacement, a small sample of 100 trees from the database of trees observed during the ground surveys. Then a coupled wind and tree resistance model (Peltola and Kellomaki 1993) determines the percentage of trees that fall in this fictitious plot for a set of wind speeds ranging from light breezes to extreme wind speeds. The model works by first calculating the lateral displacement of each tree under the influence of a particular wind-induced force, and then the resulting turning moment (or torque) at the base of the stem. If the turning moment exceeds the tree's trunk or root system resistance to breakage or overturning, the tree falls. Kretcshmann (2010) and Panshin and de Zeeuw (1970) provide the modulus of rupture and the modulus of elasticity for each species. Since values for the modulus of rupture typically represent lab-tested values for clean, knot-free wood, trunk resistance here is reduced to 85% of the ideal trunk strength, following the recommendations of Gardiner et al. (2000).

Application of the Peltola and Kellomaki (1993) tree stability model requires knowledge of the height, DBH, crown depth, and crown diameter for each tree. Since the ground surveys could not possibly measure all of these parameters, it becomes necessary to augment the measurements with estimates of tree height and crown shape for each tree. Observed tree heights are available for 788 (i.e., approximately half) of the trees surveyed in the CNF track. For all other surveyed trees, an estimate

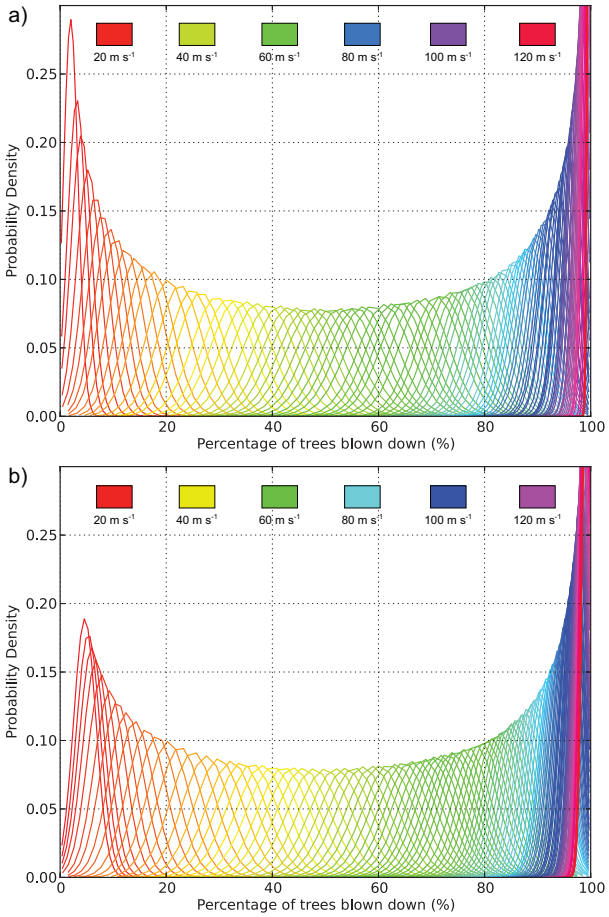

FIG. 2. Distributions of the percentage of trees blown down at various wind speeds in 10 000 fictitious sample plots using trees drawn from a database of observed trees in a) the Great Smoky Mountains National Park and b) the Chattahoochee National Forest. The color scales differ in each plot.

of tree height derives from a species-dependent height–DBH allometry (Purves et al. 2007). Comparisons between observed and estimated tree heights (not shown) indicate that the height estimates are reasonable. The ideal tree distribution model (ITD, Purves et al. 2007) determines the crown shapes within a stand of trees by selecting the height of the canopy above the ground at which the total of the exposed crown areas is equal to the ground area. The calculation accounts for the species dependence of the crown radius and crown depth for each tree. As implemented here, the ground area matches the 400 m^2 area of the ground survey plots and the ITD model calculates crown shapes for the observed trees in each plot. Therefore, each ground survey plot receives an estimate of the tree heights and crown shapes for the actual trees in that plot. Trees with a total height that is less than the calculated height of the canopy bottom receive a fixed species-dependent crown radius. In the original ITD model, these understory trees also receive a fixed crown depth. Here, understory trees receive a more reasonable estimate for crown depth of 30% of their total height. Empirical evidence based on numerous ground surveys suggests that, regardless of species, observed tree crowns constitute approximately the upper 50% of the total tree height for canopy trees, with understory crown depths of around 30%. Taken together, the DBH, height, crown radius, and crown depth allow the tree stability model to calculate the wind load on each tree.

Each wind speed increment corresponds with a particular percentage of fallen trees within each random sample of 100 trees drawn from the database of observed trees. Repeating the resampling procedure 10 000 times yields a Gaussian distribution of treefall percentages for each wind speed (Fig. 2). For example, a wind speed of 50 m s^{-1} in the GSMNP forest knocked down an average of 57.1% of the trees in each of the 10 000 random sample plots, with a range of damage between 38 and 74 of the 100 trees knocked down, and with a standard deviation of 4.98 trees.

In small sections of forest, the assignment of an EF-scale level proceeds by assessing the observed percentage of fallen trees. These subplots measure 100 m $\times$ 100 m, a scale chosen both to approximate roughly the number of trees in the fictitious plots and to provide adequate spatial coverage while still capturing spatial variations in damage severity. The most probable wind speed that produced the damage in each subplot then corresponds with the associated Gaussian probability density function (PDF) with its peak matching the observed percentage of trees blown down in that forest section (Fig. 3). To avoid undersampling, the procedure ignores subplots with 10 or fewer total trees.

4. MAPS OF EF-SCALE DAMAGE

Application of this estimation procedure to the entire length of both tornado tracks yields maps showing estimates of the EF-scale ratings based on forest damage severity (Fig. 4). The procedure also captures the variability in the intensity of each tornado along its track and appropriately assigns lower EF-scale levels on the outside edges of the damage tracks and assigns higher EF-scale levels nearer to the center of each track. Notably, both tornadoes produced damage rated EF5 by the estimation technique where nearly 100% of the trees were blown down in the small subplots. Also, a few subplots rated EF5 border subplots with ratings of EF0 or no rating at all. This result is consistent with the authors' own observations and with Blanchard (2013), who also studied forest damage from tornadoes and noted sharp spatial gradients in the level of damage within the forest. The small-scale variability also stems from the relationship between the surface flow field and the complex terrain.

Fig. 5 shows a section of the GSMNP tornado track near the intersection of the Hatcher Mountain Trail and the Little Bottoms Trail along Abrams Creek (see the inset in Fig. 4). The EF-scale ratings appear overlaid on

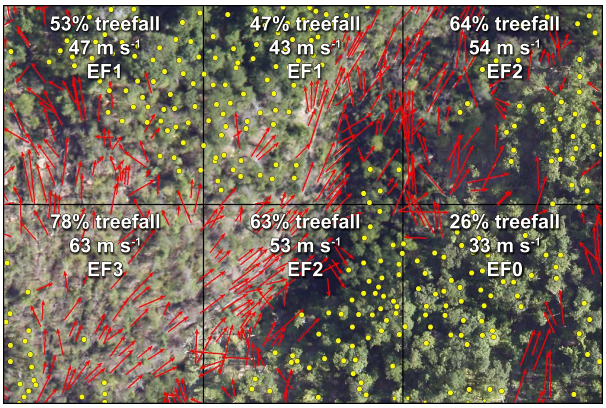

FIG. 3. A section of the GSMNP tornado track illustrating the assignment procedure for EF-scale levels. Red arrows represent fallen trees, yellow dots represent standing trees, and the black lines show the boundaries of the 100 m $\times$ 100 m subplots. At the top left, for example, the tornado knocked down 53% of the trees in the subplot, corresponding with a most probable wind speed of 47 m s^{-1} and an EF-scale rating of EF1.

the aerial imagery showing the standing and fallen trees. In this section of the forest, the tornado moved from the bottom left to the top right (i.e., northeast), first descending a mountain toward Abrams Creek, then ascending Hatcher Mountain toward the top right of the image. As the tornado crossed Abrams Creek and ran into the steep hillside, the flow likely constricted and accelerated. The tornado completely destroyed the canopy on the hillside facing the oncoming tornado (Fig. 6) and accelerated up a small valley to the north of the hill, but left the trees on the back side of the hill nearly untouched. The automated EF-scale estimation procedure captures the variability in the damage on this small scale. The technique also captures the likely wind speeds responsible for the damage, as shown in Fig. 6. Here, the lower left portion of the image corresponds with a subplot to which the estimation procedure assigned a rating of EF3 and the right two-thirds of the image corresponds with a rating of EF4. This result remains entirely consistent with the levels of damage observed in person in this area of the forest.

5. DISCUSSION

The technique described here uses tree damage severity following tornadoes or other windstorms to estimate the wind speed responsible for the damage. The results of the automated analysis remain consistent with the authors' ground observations in both tornado tracks and capture the spatial variability of the damage. Notably, the analysis requires a balanced spatial distribution of tagged trees in each subplot (i.e., approximately every nth tree must be tagged) in order to avoid corrupting the calculation of the percentage of the fallen trees within that subplot. However, application of a filtering algorithm that considers only a certain number of trees within a given area could easily solve the problem by accounting for spatial density variations resulting from two dif-

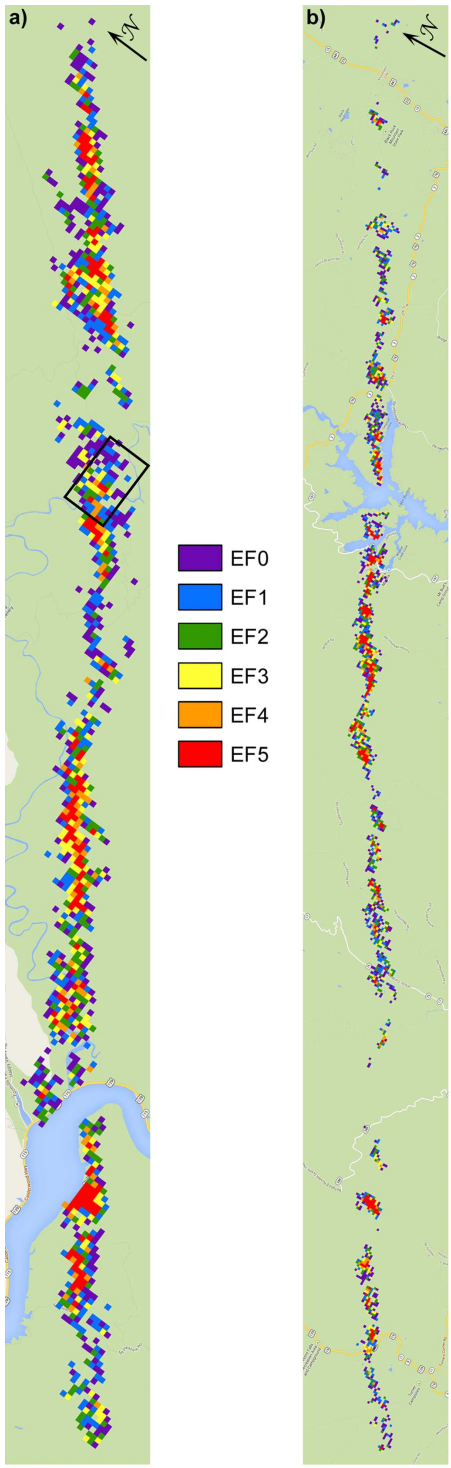

FIG. 4. Enhanced Fujita scale ratings assigned to small subplots along the length of a) the GSMNP tornado track and b) the CNF tornado track. The inset in a) is the region shown in Fig. 5. Note that the scales differ in each map. The GSMNP track is 18 miles long and the CNF track is 38 miles long.

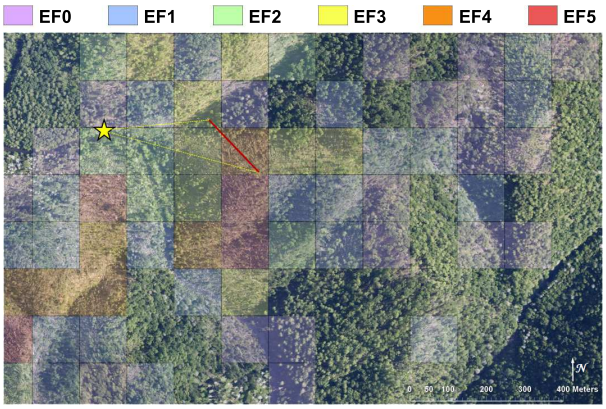

FIG. 5. EF-scale estimates near the intersection of the Hatcher Mountain Trail and the Little Bottoms Trail along Abrams Creek in the GSMNP (see inset in Fig. 4). The star indicates the location of the photographer and the red line corresponds with the field of view in the photo shown in Fig. 6.

FIG. 6. Photograph, taken 15 months after the GSMNP tornado, looking east showing a steep slope that the damage estimation technique labeled EF3 (left third) and EF4 (right two-thirds). The tornado completely destroyed the forest canopy.

ferent tree labelers or analyses viewed at different zoom levels. The wind-speed assignment procedure also assumes a uniform wind speed across each subplot, similar to the assumptions of Canham et al. (2001). This bold assumption ignores the fact that the terrain influences the near-surface tornadic flow field, as is clearly evident in Fig. 3. The assigned wind speed therefore represents a smoothed value for the wind speed in each subplot. The chosen areal coverage of the subplots, therefore, necessitates a balance between the requirement for a sufficiently large sample of trees and the requirement for sufficiently small spatial coverage to avoid excessive smoothing.

The distributions of treefall percentages for each wind speed increment depend upon the results of the tree stability model. This model in turn depends strongly on the published modulus of rupture and the modulus of elasticity for each tree species, mostly determined through laboratory studies on homogeneous, straight-grained wood. Real trees may have a different response than that given by the model when subjected to strong winds. Empirical winching studies can help to determine the mechanical properties of real trees by pulling on the trunks with a known force until they break or uproot. While this technique remains very rare in the United States, regions such as Canada, the United Kingdom, and Scandinavia practice the technique more commonly. With improved estimates of tree strength from winching studies on trees found in U.S. forests, the tree stability model could more reliably determine the fate of a particular tree at a given wind speed.

Additionally, this estimation technique easily allows for the calculation of confidence intervals on each wind speed estimate. First, each of the fictitious sample plots gets assigned a wind speed for the complete range of possible percentages of downed trees from 0% to 100%. For example, if the model knocks down 52% of the trees for a wind speed of 46 m s^{-1} and 54% of the trees for the next wind speed increment of 47 m s^{-1} in a particular sample, then the higher wind speed of 47 m s^{-1} must also knock down 53% of the trees. With this 10 000-member sampling distribution for each percentage of trees blown down, the 95% confidence interval is the range defined by the 250th and the 9750th sorted samples. For example, the most probable wind speed for an observed treefall percentage of 76% in a subplot in the GSMNP track is 62 m s^{-1} with a 95% confidence interval defined by the range 56–70 m s^{-1}. This method can therefore provide a range of possible wind speeds and EF-scale levels responsible for a given degree of forest damage.

This approach may lead to methods for straightforward estimation of EF-scale levels in remote or inaccessible locations. In order to provide useful EF-scale estimates in a short time frame, the method requires speedy acquisition of high-resolution aerial photographs. Ideally, an automated tree-tagging algorithm could quickly process the georeferenced imagery and determine the location of both standing and fallen trees. Additionally, wind speed estimates that correspond with various degrees of forest damage would require representative samples of the tree species and size composition obtained from ground surveys in various forested regions.

Acknowledgments. The authors wish to thank Michael Goldsbury and Dawn Pomeroy for tagging nearly half a million trees in their spare time and the National Park Service and U.S. Forest Service for granting access to remote regions of the Great Smoky Mountains National Park and the Chattahoochee National Forest. This work benefited from data acquired during a project funded by NSF RAPID grant AGS-1141926.

REFERENCES

Bech, J., M. Gayà, M. Aran, F. Figuerola, J. Amaro, and J. Arús, 2009: Tornado damage analysis of a forest area using site survey

observations, radar data and a simple analytical vortex model. *Atmos. Res.*, **93,** 118–130.

Beck, V., and N. Dotzek, 2010: Reconstruction of near-surface tornado wind fields from forest damage. *J. Appl. Meteor. Climatol.*, **49,** 1517–1537.

Blanchard, D. O., 2013: A comparison of wind speed and forest damage associated with tornadoes in Northern Arizona. *Wea. Forecasting,* **28,** 408–417.

Bluestein, H. B., 2000: A tornadic supercell over elevated, complex terrain: The Divide, Colorado, storm of 12 July 1996. *Mon. Wea. Rev.*, **128,** 795–809.

Bosart, L. F., A. Seimon, K. D. LaPenta, and M. J. Dickinson, 2006: Supercell tornadogenesis over complex terrain: The Great Barrington, Massachusetts, tornado on 29 May 1995. *Wea. Forecasting,* **21,** 897–922.

Canham, C. D., M. J. Papaik, and E. F. Latty, 2001: Interspecific variation in susceptibility to windthrow as a function of tree size and storm severity for northern temperate tree species. *Can. J. For. Res.*, **31,** 1–10.

Dessens, J., 1972: Influence of ground roughness on tornadoes: A laboratory simulation. *J. Appl. Meteor.*, **11,** 72–75.

Dunn, L. B., and S. V. Vasiloff, 2001: Tornadogenesis and operational considerations of the 11 August 1999 Salt Lake City tornado as seen from two different Doppler radars. *Wea. Forecasting,* **16,** 377–398.

Fiedler, B. H., 1994: The thermodynamic speed limit and its violation in axisymmetric numerical simulations of tornado-like vortices. *Atmos.–Ocean,* **32,** 335–359.

——, and R. Rotunno, 1986: A theory for the maximum windspeeds in tornado-like vortices. *J. Atmos. Sci.*, **43,** 2328–2340.

Fujita, T. T., 1989: The Teton-Yellowstone tornado of 21 July 1987. *Mon. Wea. Rev.*, **117,** 1913–1940.

Gardiner, B., H. Peltola, and S. Kellomaki, 2000: Comparison of two models for predicting the critical wind speeds required to damage coniferous trees. *Ecological Modelling,* **129,** 1–23.

Godfrey, C. M., and C. J. Peterson, 2012: Reconstruction of near-surface tornado wind fields from forest damage patterns in complex terrain. Preprints, *26th Conference on Severe Local Storms*, Nashville, TN, Amer. Meteor. Soc., P115.

Holland, A. P., A. J. Riordan, E. C. Franklin, 2006: A simple model for simulating tornado damage in forests. *J. Appl. Meteor. Climatol.*, **45,** 1597–1611.

Karstens, C. D., W. A. Gallus, B. D. Lee, and C. A. Finley, 2013: Analysis of tornado-induced tree fall using aerial photography from the Joplin, Missouri, and Tuscaloosa–Birmingham, Alabama, Tornadoes of 2011. *J. Appl. Meteor. Climatol.*, **52,** 1049-1068, doi:10.1175/JAMC-D-12-0206.1.

Kretschmann, D. E., 2010: Mechanical properties of wood. *Wood Handbook: Wood as an Engineering Material.* General Technical Report FPL-GTR-190, U.S. Department of Agriculture, Forest Service, Forest Products Laboratory, 508 pp.

LaPenta, K. D., L. F. Bosart, T. J. Galarneau, and M. J. Dickinson, 2005: A multiscale examination of the 31 May 1998 Mechanicville, New York, F3 tornado. *Wea. Forecasting,* **20,** 494–516.

Letzmann, J. P., 1925: Advancing air vortices. *Meteor. Z.*, **42,** 41–52.

Lewellen, D. C., and W. S. Lewellen, 2007: Near-surface intensification of tornado vortices. *J. Atmos. Sci.*, **64,** 2176–2194.

——, ——, and J. Xia, 2000: The influence of a local swirl ratio on tornado intensification near the surface. *J. Atmos. Sci.*, **57,** 527–544.

——, Baiyun Gong, and W. S. Lewellen, 2008: Effects of finescale debris on near-surface tornado dynamics. *J. Atmos. Sci.*, **65,** 3247–3262.

Lewellen, W. S., D. C. Lewellen, and R. I. Sykes, 1997: Large-eddy simulation of a tornado's interaction with the surface. *J. Atmos. Sci.*, **54,** 581–605.

Panshin, A.J., and C. de Zeeuw, 1970: *Textbook of Wood Technology.* 3rd ed. McGraw-Hill, 705 pp.

Peltola, H., and S. Kellomaki, 1993: A mechanistic model for calculating windthrow and stem breakage of Scots pine at stand edge. *Silva Fennica,* **27,** 99–111.

Purves, D. W., J. W. Lichstein, and S. W. Pacala, 2007: Crown plasticity and competition for canopy space: A new spatially implicit model parameterized for 250 North American tree species. PLoS ONE, 2(9), e870, doi:10.1371/journal.pone.0000870.